

Linking coordinative and executive dysfunctions to atrophy in spinocerebellar ataxia 2 patients

Federico D'Agata · Paola Caroppo · Andrea Boghi · Mario Coriasco · Marcella Caglio · Bruno Baudino · Katuscia Sacco · Franco Cauda · Elisabetta Geda · Mauro Bergui · Giuliano Geminiani · Gianni Boris Bradac · Laura Orsi · Paolo Mortara

Received: 23 December 2010 / Accepted: 13 March 2011
© Springer-Verlag 2011

Abstract Spinocerebellar ataxias type 2 (SCA2) is a rare genetic disorder characterised by the degeneration of the Cerebellum, its connections and many Brainstem areas. A voxel-based morphometry (VBM) analysis was performed on 12 genetically determined SCA2 patients and 31 controls, normalising the brains with two different atlases: one was created in-house with DARTEL (a diffeomorphic registration method) and the other was SUIT (an exclusive

Cerebellum atlas). We administered two versions of a popular executive/planning functions test: the Tower of London, in the traditional and in a computerised version that does not require the use of hands, to correlate the regional atrophy with the tests' performances and to discover the different associations of Cerebellum's areas to cognitive dysfunctions. SCA2 showed a diffuse infratentorial atrophy with the whole Cerebellum and Brainstem affected, the overall patterns were highly overlapping between atlases with some minor differences. The DARTEL VBM also allowed detecting two supratentorial clusters of atrophy, one in the left Inferior Parietal Lobule and the other in the Corticospinal Tracts. Additional analyses revealed a partial involvement of many White Matter tracts and of the Thalamus in the pathology. The classical Tower of London version correlated maximally with the right Lobule IV–V, when the computerised version correlated with the right Crus 1. The correlations of different versions of the test suggested a dissociation between the dysfunctions in SCA2: the Posterior Cerebellum was linked to the executive dysfunction while the Anterior Cerebellum was linked to the coordinative dysfunction.

F. D'Agata and P. Caroppo contributed equally to this work.

Electronic supplementary material The online version of this article (doi:10.1007/s00429-011-0310-4) contains supplementary material, which is available to authorized users.

F. D'Agata · P. Caroppo · M. Coriasco · M. Caglio · M. Bergui · G. B. Bradac · L. Orsi · P. Mortara
Department of Neuroscience,
AOU S. Giovanni Battista, Turin, Italy

F. D'Agata · M. Caglio · K. Sacco · F. Cauda · E. Geda · G. Geminiani
Department of Psychology, University of Turin, Turin, Italy

F. D'Agata · K. Sacco · F. Cauda · E. Geda · G. Geminiani
CCS-fMRI, Koelliker Hospital, Turin, Italy

A. Boghi
Section of Neuroradiology, Department of Radiodiagnostics,
ASO S. Croce, Cuneo, Italy

B. Baudino
Nuclear Medicine, AOU S. Giovanni Battista, Turin, Italy

K. Sacco · G. Geminiani · P. Mortara
NIT, Neuroscience Institute of Turin, Turin, Italy

F. D'Agata (✉)
Department of Neuroscience, University of Turin,
Via Cherasco, 15, 10126 Turin, Italy
e-mail: federico.dagata@unito.it

Keywords Cerebellum · Cerebellar atrophy · Spinocerebellar ataxia · SCA · SCA2 · Type 2 · Voxel-based morphometry · VBM · Tower of London

Abbreviations

ADCA	Autosomal dominant cerebellar ataxia
CSF	Cerebrospinal fluid
FWE	Family Wyse error
FWHM	Full width half maximum
FDR	False discovery rate
GM	Grey matter
ICARS	International Cooperative Ataxia Rating Scale

MMSE	Mini mental state examination
MNI	Montreal Neurological Institute
MRI	Magnetic resonance imaging
NS	Not significant
SCA	Spinocerebellar atrophy
SD	Standard deviation
SE	Standard error
TIV	Total intracranial volume
ToL	Tower of London
CPU	Tower of London computerised version
PEG	Tower of London Pegs version
VBM	Voxel-based morphometry
WM	White matter

Introduction

Autosomal dominant cerebellar ataxias (ADCA), referred to as spinocerebellar ataxias (SCAs) in genetic nomenclature, are a clinically and genetically heterogeneous group of rare neurodegenerative disorders characterised by the slow degeneration of the Cerebellum and its connections, often accompanied by degenerative changes in the Brainstem and elsewhere (Dürr 2010; Schöls et al. 2004; Soong and Paulson 2007). Overall, SCAs have a prevalence of 1–3/100,000 in Europe (Dürr 2010). At present there are at least 29 subtypes of SCA identified (Dürr 2010; Schöls et al. 2004); SCA2 represents the most frequent genotype (24%) in Italian ADCA kindred (Brusco et al. 2004; Schöls et al. 2004). Its pathogenesis relies on CAG repeats expansion in the affected gene (12q24), clinically the phenotype is highly variable and comprises ataxia with slow saccades, peripheral neuropathy and less frequent extrapyramidal findings. The age at onset is most commonly in the third–fourth decade, it is inversely correlated with the repeat length, and it shows the anticipation phenomenon (Schöls et al. 2004). The disease has generally a progression to the loss of physical control, disability and death, with a relative retains of mental capacities, although the presence of cognitive alterations (especially verbal memory and executive dysfunction) is a common findings (Bürk et al. 1999; Bürk et al. 2003; Bürk 2007; Klinke et al. 2010; Le Pira et al. 2002) and dementia is reported from 15 to 25% depending on the stage of the disease (Bürk et al. 1999; Orsi et al. 2010).

Three neuropathological studies (a total of 15 patients, 11 from Cuba, 2 from Martinique, 1 from USA, 1 not specified) found extreme loss of pontine and olivary nuclei and Purkinje cells, with relative preservation of the dentate nuclei and cerebral cortex, the spinal cord was reported as severely affected (Dürr et al. 1995; Estrada et al. 1999; Pang et al. 2002). Two other neuropathological studies

(five patients from Germany) reported also a thalamic nuclei involvement (Rüb et al. 2003a, b, 2005).

Voxel-based morphometry (VBM), introduced by Ashburner and Friston (2000), consisted, at its simplest version, in a voxel-wise comparison of the local concentration of Grey Matter (GM) between two groups of subjects. This procedure involved spatially normalising high-resolution images from all the subjects in the study into the same stereotactic space. This is followed by segmenting the GM from the spatially normalised images and smoothing the GM segments. Voxel-wise parametric statistical tests, which compare the smoothed GM images from the two groups, were performed to discover local differences in GM concentration. Good et al. (2001) proposed a change in the workflow processing, the so-called Optimised VBM. Separate Grey and White Matter (WM) templates were created from an initial simple VBM analysis and then the templates were used to optimally normalise the images that were segmented again before the parametric statistical tests. Moreover, in order to preserve the volume of a particular tissue (GM or WM) within a voxel, a further processing step was incorporated, the multiplying (or modulating) voxel values in the segmented images by the Jacobian determinants derived from the spatial normalisation step. Ashburner and Friston (2005) proposed the Unified Segmentation (implemented in SPM5 and in SPM8), a probabilistic framework that enables image registration, tissue classification, and bias correction to be combined within the same generative model, to resolve the inherent circularity of the Optimised VBM, in fact the steps, instead of being done in a iterative sequence, are components of a single model. Ashburner (2007) introduced Diffeomorphic Anatomical Registration Through Exponentiated Lie Algebra (DARTEL), which is a fast algorithm for diffeomorphic images registration; the idea, behind adding DARTEL in the VBM workflow, is to increase the accuracy of inter-subject alignment by modelling the shape of each brain using millions of parameters (three parameters for each voxel). DARTEL works by aligning GM among the images, while simultaneously aligning WM. This is achieved by generating its own increasingly crisp average template data, to which the data are iteratively aligned. DARTEL has demonstrated to improve the VBM results in the majority of studies where it has been employed and compared with previous methods (Bergouignan et al. 2009; Cuingnet et al. 2010; Klein et al. 2009; Pereira et al. 2010).

Another way to improve the inter-subjects alignment in Cerebellum VBM is the employment of the Spatially Unbiased Infratentorial Template (SUIT) of Diedrichsen (2006), Diedrichsen et al. (2009). SUIT is a new high-resolution atlas template of the human Cerebellum and Brainstem in the MNI stereotactic space. The analysis is

more accurate, but is confined to the Cerebellum and Brainstem.

The Tower of London (ToL) is a popular neuropsychological test for the assessment of executive functions and Working Memory (Shallice 1982). Executive functions refer to the goal-directed planning abilities, which include decision-making, strategy formation, organisation and sequencing of mental functions. Functional studies demonstrated the activation of a fronto-parietal-occipital network including the Dorsolateral Prefrontal cortex, and the Inferior Parietal Lobe during a ToL task and decision-making task (Schall et al. 2003; Andreasen et al. 1992; Morris et al. 1993; Baker et al. 1996; Dagher et al. 1999; Lazeron et al. 2000; Fincham et al. 2002; Newman et al. 2003; Van den Heuvel et al. 2003; Rasser et al. 2005). Boghi et al. (2006) showed that highly significant increases of activation in frontal, parietal, occipital cortical areas and in cerebellar hemispheres were associated with the performance of the task confirming previous SPECT, PET and fMRI studies.

The classical version of this test requires not only executive abilities but also visuospatial abilities and a fine coordinate visuomotor manipulation (ToL PEG). We realised a computerised version (ToL CPU) that can be solved without any complex hands or eyes motor control (Boghi et al. 2006), more correct for the investigation of patients with motor disorders. Neither of the two tests can be regarded as pure measure of executive functioning, as both tests involve different other domains in their task performance as Working Memory, Arithmetic Skill, Attention and Visuospatial Memory. Moreover, the load of the different components could be different between the two tests.

Aim of the study

In this study, first, we characterised the atrophy pattern of SCA2 patients, in comparison with healthy controls, to validate our SPM results respect the VBM studies taken from the scientific literature (Brenneis et al. 2003; Della Nave et al. 2008a, b). Then, we correlated the performances in the two versions of ToL with SCA2 atrophy to demonstrate a possible dissociation of the areas of atrophy associated with a prevalent coordinative (ToL PEG) or executive dysfunction (ToL CPU).

An additional aim was the comparison between the results obtained employing different methods: DARTEL and SUIT.

Methods

All statistical analyses, when not specified, were implemented on SPSS 13TM software statistical package (SPSS Inc., Chicago, USA; <http://www.spss.com>).

Subjects

Twelve right-handed patients (10 males, mean \pm SD age = 48 ± 10 years, demographic and clinical data in Table 1) with genetically defined SCA2 (Nardacchione et al. 1999) were recruited at the Center for Spinocerebellar Ataxia Diseases—AOU S. Giovanni Battista, Turin, Italy and underwent a brain MRI. Cerebellar ataxia was scored by ICARS, an international validated clinical scale for ataxia (Schmitz-Hübsch et al. 2006; Trouillas et al. 1997).

A group of 31 right-handed healthy controls of similar age ($p = 0.49$, 12 males, mean \pm SD age = 45 ± 11 years, demographic data in Table 1), without history of alcohol or substance abuse and neurological or psychiatric disorder, were enrolled. At the time of the study, neither patients nor controls followed any kind of pharmacological treatment. The study protocol was approved by the Ethical Committee of the Turin AOU S. Giovanni Battista and all the subjects gave their written informed consent to the study and the further use of their anonymous data.

Table 1 Demographics and clinical data

Genetic type	Controls	SCA2	<i>p</i>
Number	31	12	–
Families	30	9	–
M/F	12/19	10/2	
Age (years)	45 \pm 11	48 \pm 10	0.49
Educational level (years)	15 \pm 4	9 \pm 3	<0.01
MMSE ($n \leq 23.8$)	28.5 \pm 0.5 (0)	26.8 \pm 1.8 (0)	0.05
Forebrain GM/TIV	0.38 \pm 0.03	0.38 \pm 0.03	0.74
Tower of London PEG	27 \pm 4	21 \pm 4	<0.01
Max 36 and % Max	77 \pm 13	58 \pm 21	<0.01
Tower of London CPU	32 \pm 6	22 \pm 9	<0.01
Max 41 and % Max	79 \pm 15	55 \pm 24	<0.01
SDS Zung ($n \geq 50$)	–	47 \pm 9 (7)	–
Onset age (years)	–	37 \pm 10	–
Disease duration (years)	–	11 \pm 5	–
Triplet CAG repeats	–	39 \pm 2	–
Range		36–41	
ICARS total (/100)	–	29 \pm 5	–
Posture and gait (/34)	–	9 \pm 2	–
Kinetic functions (/52)	–	16 \pm 3	–
Speech (/8)	–	3 \pm 1	–
Oculomotion (/6)	–	2 \pm 1	–
Stage	–	1.2 \pm 0.4	–

Stage 1: onset of gait difficulties; Stage 2: loss of independent gait; Stage 3: confinement to wheelchair (Klockgether et al. 1998)

For cognitive impairment MMSE cut-off = 23.8, corrected for age and education. For depression SDS Zung cut-off = 50

Mean \pm standard deviation; *p* for 2 sample *t* test, in bold $p < 0.05$

Neuropsychological assessment

A neuropsychologist administered MMSE (Folstein et al. 1975) to exclude subjects below the cut-off of 23.8 score corrected for subject's age and education (Measso et al. 1993). Depression was scored using Zung (1965) Self-Rating Depression Scale (SDS) a 20-item self-report questionnaire that is widely used as a screening tool, covering affective, psychological and somatic symptoms associated with depression. Most people with depression score between 50 and 69, while a score of 70 and above indicates severe depression.

Then he administered the two versions of ToL. The PEG version uses a board with three pegs of different length (Fig. 1, upper left) and three coloured spheres. The test consists in solving, in a fixed number of moves, 12 puzzles, going from a start position (Fig. 1, lower left) to a goal position (e.g. Fig. 1, lower right), moving only one sphere at a time from one peg to another. The test is scored on the basis of the time of solution of the puzzles, 6 are easy problems with a maximum resolution time of 30 s and 6 are difficult problems with a maximum time of 60 s. The maximum score is 36. The CPU version (Fig. 1, upper right) uses a picture with coloured circles and three vertical lines representing spheres and pegs, the figure is split in two parts, the upper half shows the start position and the lower half the goal position. The test consists in answering what is the minimum number of moves to go from start to goal moving one circle at time from one line to another. The picture is static so the subjects need to mentally imagine the in-between moves. The test has 20 puzzles and is scored on the basis of the number of correct answers, 10 problems are easy with a maximum time of 15 s to answer and 10 are difficult with a maximum time of 30 s. The score for every problem depends on difficulty and it is proportional to the number of in-between moves needed to keep in mind. The maximum score is 41. All tests were administered during a single session in the day of the MRI scan. The paradigm followed this sequence: First, in a room free of noise and without interruption, we administered PEG version. A 10-min training preceded the administration of the CPU version. Parallel and equivalent forms were used for training session. We spend approximately 20 min between the administration of the PEG and CPU versions.

MRI data acquisition

All the structural MRI scans of all participants were acquired on a 1.0 T Impact Magnetom ImagerTM scanner (Siemens, Erlangen, Germany). Whole brain scans were obtained as high-resolution T1-weighted 3D MP-RAGE (Magnetisation Prepared Rapid Acquisition Gradient

Echo), acquired in the sagittal plane (TR = 11.4 ms, TE = 4.4 ms, TI = 300 ms, FA = 15°, FOV = 250 mm × 250 mm, 256 × 256 in-plane matrix, 128 slices of 1.5 mm thickness).

VBM analysis

Images analysis was performed on a workstation using the Statistical Parametric Mapping package (SPM8, rel. lug-10, <http://www.fil.ion.ucl.ac.uk/spm>) in MATLAB 7.5TM environment (Math Works Inc., Natick, MA, USA; <http://www.mathworks.com>). We took the following 1–4 steps for both DARTEL and SUIT workflows:

1. Check for scanner artefacts and gross anatomical abnormalities for each subject.
2. Set image origin at the Anterior Commissure AC.
3. Use the Unified Segmentation toolbox to segment the images in GM and WM partitions (see Supplementary Fig. 1).
4. Reslice the images with a trilinear interpolation algorithm to an isotropic voxel of 1 mm × 1 mm × 1 mm.

Then we normalised, in a different way, for the two methods in the final steps:

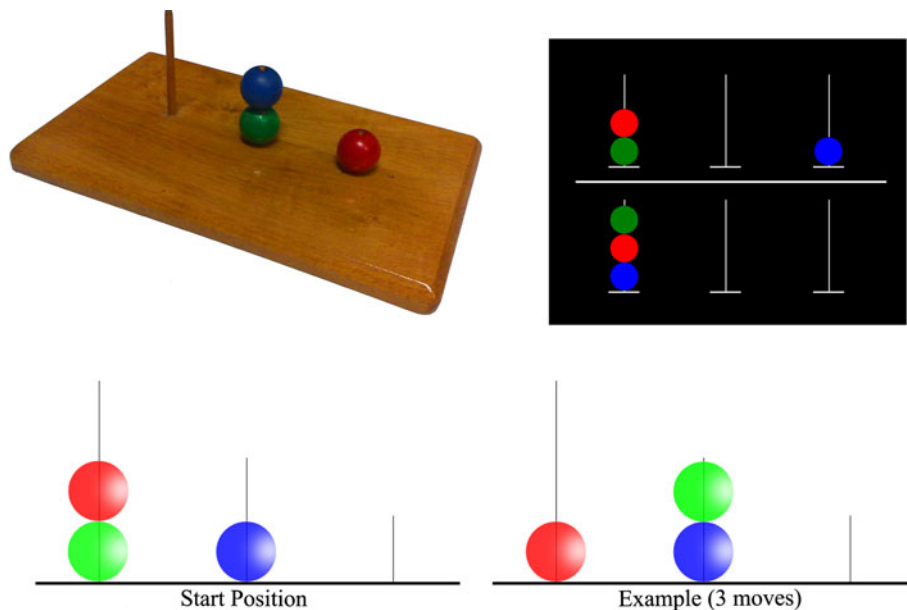
DARTEL

5. Use DARTEL toolbox to have a high-dimensional normalisation protocol (see the resulting template in Supplementary Fig. 2). We followed John Ashburner's chapter in its standard version including the MNI space transformation.
6. Check for homogeneity across sample and use the standard version of the smoothing (i.e. 8 mm FWHM isotropic Gaussian kernel, Supplementary Fig. 3 left).

SUIT

5. Use SUIT 2.5 an SPM extension (<http://www.icn.ucl.ac.uk/motorcontrol/imaging/suit.htm>) to isolate the Cerebellum and generate the segmentation maps.
6. Hand correct the isolated map if necessary, excluding any GM included outside the Cerebellum: exclusive mask were drawn with MRICron (<http://www.cabiatl.com/mricro/mricron/index.html>) and SPM Image Calculator used to exclude the outside voxels.
7. Normalise the cropped anatomical images and reslice the segmentation map into SUIT atlas space (e.g. Supplementary Fig. 4).

Fig. 1 Tower of London test materials. *Upper left* tower of London pegs-board (ToL PEG), *upper right* difficult trial of the computerised Tower of London (ToL CPU), the answer is 6 moves to go from start to goal positions, *lower left* start position for all the ToL PEG trials, *lower right* an example of an easy ToL PEG trial (goal position for 3 moves)



8. Check for homogeneity across sample and use a lesser smoothing to preserve precision in the definition of cerebellar structures (i.e. 4 mm FWHM isotropic Gaussian kernel, Supplementary Fig. 3 right).

After this pre-processing we obtained smoothed modulated normalised data of $1 \text{ mm} \times 1 \text{ mm} \times 1 \text{ mm}$ voxels for DARTEL ($181 \times 217 \times 181$ voxels) and SUIT ($141 \times 95 \times 87$ voxels) that we used for the statistical analysis.

Regions of interest analysis

We used MarsBar (Brett et al. 2002), an SPM extension for Regions of Interest (ROIs) analysis, to make statistical inferences on normalised unsmoothed data limited to some cortical and subcortical areas. Moreover we created masks from 25 GM (Anterior Cingulate Cortex, Brainstem, Caudate, Cerebellum, Dorsolateral Prefrontal Cortex, Inferior Parietal Lobule, lateral Orbito Frontal Cortex, Primary Motor Cortex, Middle Cingulate Cortex, Medulla, Medial Frontal Cortex, Midbrain, medial Orbito Frontal Cortex, Pallidum, Posterior Cingulate Cortex, Pons, Putamen, Red Nucleus, Primary Sensorial Cortex, Supplementary Motor Area, Superior Parietal Lobule, Superior Temporal Gyrus, Thalamus, Primary Visual Cortex, Ventrolateral Prefrontal Cortex) and 22 WM ROIs (Body of Callosum, Brainstem, Callosum, Cingulum, Corticospinal Tract, Genu Callosum, Inferior Cerebellar Peduncles, Inferior Occipital Fascicle, High Corticospinal Tract, Low Corticospinal Tract, Middle Cerebellar Peduncles, Medium Corticospinal Tract, Medulla, Midbrain, Optic Radiation, Pons, Pontine Crossing Tract, Superior Cerebellar Peduncles, Superior Longitudinal Fascicle, Superior Occipital Fascicle, Splenium of Callosum, Uncinate Fascicle) using MarsBar to

convert ROIs from marsbar-aal-0.2 (<http://marsbar.sourceforge.net/download.htm>), Fibers v. 15 Anatomy Toolbox (http://www.fz-juelich.de/inm/inm-1/spm_anatomy_toolbox) (Eickhoff et al. 2005) and ICBM labelled template (<http://www.loni.ucla.edu/Atlases>). We backprojected the masks (e.g. Supplementary Fig. 5) from MNI space into the native space of the subjects using the inverted deformation from standard space to subject space derived from Unified Segmentation toolbox and we extracted the partial GM, WM volumes from masks with the Ged Ridgway's get_totals matlab function (http://www.cs.ucl.ac.uk/staff/g.ridgway/vbm/get_totals.m) that gives the total volume of voxels above a given relative threshold (we used 1%) inside a specified mask.

For the estimation of Total Intracranial Volume (TIV) of subjects we used a robust method (Keihaninejad et al. 2010) that backproject the GM + WM + CSF tissue probability maps (10% thresholded) into native space to extract the volume.

Groups comparisons

We used independent two tailed two samples *t* test (equal or not equal variance assumed on the basis of a Levene's test) to compare means of demographic and neuropsychological scores of controls and SCA2. We also used an ANCOVA model with TIV, age and education as covariate and genotypes as factor to compare the Tower of London scores.

An ANCOVA model with age, sex, education, TIV as covariates and genotypes as two factor levels (SCA2, controls) was estimated with SPM8 for GM atrophy (no global normalisation and no grand mean scaling). We used an identical model to test WM atrophy. We tested two

contrasts: controls > SCA2 and SCA2 > controls. We used these models on DARTEL (43 GM + 43 WM whole brain 8 mm smoothed modulated normalised images), SUIT (43 GM + 43 WM Cerebellum and Brainstem 4 mm smoothed modulated normalised images) and ROIs data (25 GM ROIs + 22 WM ROIs).

All the contrasts SPM maps were thresholded at an uncorrected $p < 0.001$. We make an additional request, to minimise false positives, to consider a voxel significant it should also belong to a cluster with a corrected cluster-level $p_{\text{corr}} \leq 0.05$, FWE corrected, by applying the Random Field Theory (Kiebel et al. 1999), for infratentorial clusters or FDR corrected (Benjamini et al. 2001) for supratentorial clusters. We used a more permissive cluster-level threshold only for extra-cerebellar voxels (as in Brenneis et al. 2003).

In the ROIs analysis we used the step-down Finner formula (FWE correction) to choose the significant group comparisons at ROIs level $p_{\text{corr}} < 0.05 : p_{\text{corr}} = 1 - (1 - p_i)^{\frac{\alpha}{n}}$, where i is the i th smallest p value in the list and n are the number of considered comparisons (Finner 1990, 1993).

Correlations

Multiple regression models with age, sex, TIV and one variable of interest were estimated with SPM8 (no global normalisation and no grand mean scaling) for GM atrophy correlations with clinical, demographic, genetic and neuropsychological parameters. The considered variables of interest were: disease duration, ICARS total score, CAG repeats, ToL PEG and ToL CPU, we tested all these one by one on DARTEL (43 GM + 43 WM whole brain 8 mm smoothed modulated normalised images) and SUIT (43 GM + 43 WM Cerebellum and Brainstem 4 mm smoothed modulated normalised images) data. We considered as significant voxels with an uncorrected $p < 0.001$ belonging to a cluster $p_{\text{corr}} \leq 0.05$ cluster-level corrected (FWE corrected for infratentorial voxels and FDR corrected for supratentorial voxels).

We calculated with the Pearson's coefficient r the table of correlations between ROIs volumes (TIV normalised), ToL PEG, ToL CPU, demographics, CAG repeats and clinical parameters (means and SDs reported in Table 1). We used the step-down Finner formula (FWE correction) (Finner 1990, 1993) to determinate the significant correlations. To confirm our data we also tested some correlation that was already consistently reported in literature.

Labelling

Statistically significant peaks were topographically labelled using MRIcron together with the AAL (Automated

Anatomical Labelling) template (Tzourio-Mazoyer et al. 2002) for forebrain GM, the Schmahmann's human cerebellar atlas (Schmahmann et al. 1999) for the Cerebellum GM and the ICBM-DTI-81 atlas (<http://www.loni.ucla.edu/Atlases>) (Mori and van Zijl 2007) for WM.

Choosing controls and covariates

For the choice of the controls group composition, we followed the suggestion of Pell et al. (2008). A difference in group sex composition and education was apparent (Table 1), but we preferred to include all the controls images in our possession to maximise the power of our analysis, instead of using a subset of better matched controls because, empirically, it could be better to increase the size of the controls group instead of matching perfectly the controls with the patients group. To verify that our choice is at least as good as having a more matched controls group we also performed all the analyses with two differently composed controls groups. We used also a sex matched controls group and an education matched controls group (see Supplementary Table 1).

For the covariates to be controlled in the modelling, we inserted sex and age as they are important confounding in volumetric studies; we also added TIV as suggested by Pell et al. (2008) and education that could have a potential impact on executive tests performance (i.e. Tower of London) and therefore could explain some of the variance.

Results

Table 1 shows SCA2 patients and controls clinical and demographic data. All the patients were over the MMSE cut-off and did not have a severe depressive condition or late stage of the disease.

The composition of controls group did not change the results of comparisons and correlations as we verified. For an example see Supplementary Fig. 6 and Supplementary Table 2 where we compared the overlapping of the three different groups comparisons for GM atrophy.

Groups comparisons

The two groups differed ($p < 0.01$, t test) for scores in ToL PEG and ToL CPU (when expressed in percent of maximum score the performances at PEG and CPU where very similar intra group, Fig. 3 Upper left and right). The difference was confirmed by the ANCOVA model (PEG, genotype $p = 0.001$ adjusted $r^2 = 0.41$; CPU, genotype $p = 0.01$ adjusted $r^2 = 0.41$).

The GM and WM atrophy patterns were described in Fig. 2, Supplementary Figs. 7–13; statistical peaks in

Table 2 for GM and Table 3 for WM; clusters gyral description in Supplementary Table 3 for GM and fascicle involvement in Supplementary Table 4 for WM. DARTEL and SUI gives a similar atrophy description with the whole Cerebellum, cerebellar peduncles and Brainstem involved (Supplementary Tables 3, 4).

The pattern included: Lobules III–VI, Crus I–II, VIIb, VIII–X, Vermis I–X, Inferior/Middle/Superior Cerebellar Peduncles, Medulla, Midbrain, Pons, Medial Lemniscus and Pontine Crossing Tract. The atrophy extended with a number of voxels over the threshold of nearly 50% in the left and 50% in the right hemisphere (for both DARTEL and SUI, see Supplementary Table 3). The atrophy extended slightly more in the Anterior Cerebellum compared to the Posterior (for both DARTEL and SUI, see Supplementary Table 3). The maximum GM peaks differed for DARTEL and SUI, where the order from max to min was Brainstem, Bilateral Posterior Cerebellum and Right Anterior Cerebellum for DARTEL (Table 2, Supplementary Table 3) and Brainstem, Right Anterior Cerebellum, and Bilateral Posterior Cerebellum for SUI (Table 2, Supplementary Table 3). Both methods gave the same peak for WM: Right Middle Cerebellar Peduncles (Table 3).

Diffeomorphic Anatomical Registration Through Exponentiated Lie Algebra showed more extended clusters of atrophy, especially in Posterior Cerebellum, but also more

voxels outside the GM atlas mask (Supplementary Table 3).

Additionally only DARTEL can show significant voxels outside Cerebellum and, indeed, there were several: in the Left Inferior Parietal Lobule (see Table 2 and Supplementary Fig. 12) and along the Cortico Spinal Tracts (they agreeably followed the a priori known shape of the fascicle, see Table 3; Fig. 2, lower right and Supplementary Fig. 13).

Regions of Interest analysis (Supplementary Table 5) showed significant differences in GM (Finner step-down corrected) for: whole Cerebellum, whole Brainstem, Midbrain, Medulla, Pons and Thalamus. In WM for: whole Brainstem, Inferior/Middle/Superior Cerebellar Peduncles, Pontine Crossing Tract, Medulla, Pons, Inferior Occipital Fascicle, Superior Longitudinal Fascicle, Uncinate Fascicle, Corticospinal Tract (especially the Low part, as we divided the Corticospinal Tract in three, approximately equal, parts along the infero-superior direction: Low, Medium and High).

Correlations

We did not find any significant correlation with SPM8 for ICARS, CAG repeats and duration of the disease. We found a striking correlation with the two version of ToL (Fig. 3, Supplementary Fig. 14, 15, 16; Table 4,

Fig. 2 VBM comparison between controls and SCA2 patients. *Upper left* SCA2 versus controls GM comparison for DARTEL normalised data, SPM maps projected onto a 3D render of the template created by DARTEL, *upper right* SCA2 versus controls GM comparison for SUI normalised data, SPM maps projected onto a 3D render of the SUI template, *lower left* SCA2 versus controls WM comparison for SUI normalised data, SPM maps projected onto 3 orthogonal planes of the SUI template, *blue cross* on the global maxima, *lower right* SCA2 versus controls WM comparison for DARTEL normalised data, projected onto 3 orthogonal planes of the Colin27 template, *blue cross* on the global maxima, detail of the Corticospinal Tracts involvement. For all the contrasts, the threshold was $p < 0.001$ uncorrected

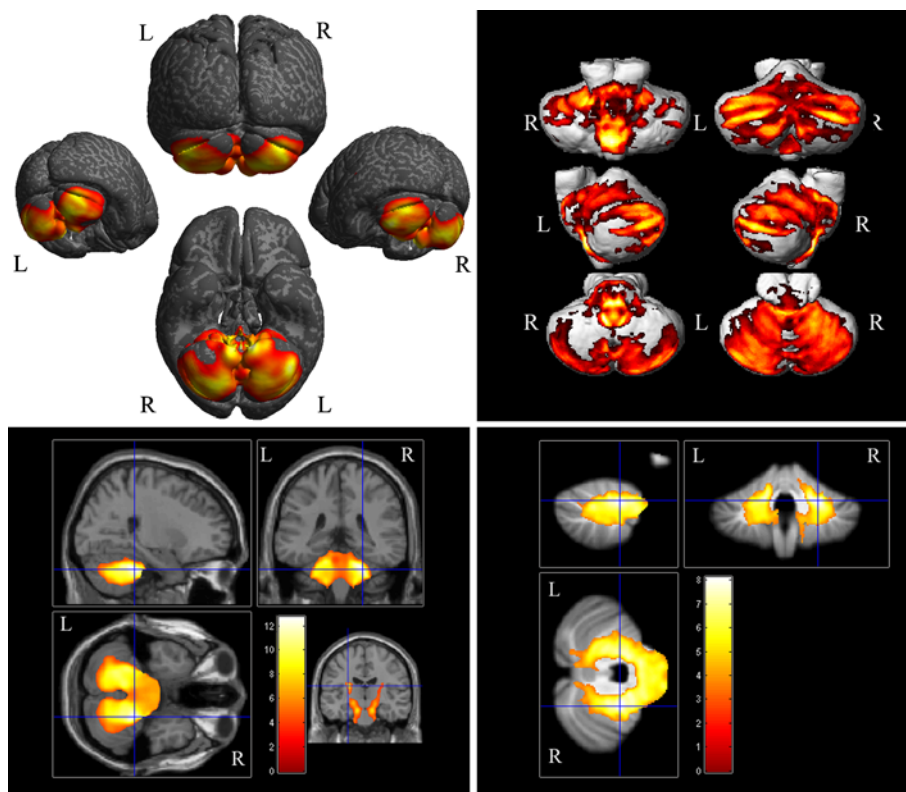


Table 2 SCA and controls GM comparison

N	DARTEL	K_e	Z_e	MNI			N	SUIT	K_e	Z_e	MNI		
				x	y	z					x	y	z
1	Med R	1,87,473	7.26	2	-48	-58	1	Med R	98,856	6.07	5	-30	-56
	VIIb L		7.18	-35	-59	-45		IV-V R		5.84	22	-49	-15
	IX L		7.18	-6	-45	-60		Med L		5.76	-4	-28	-44
	C1 L		7.02	-25	-70	-29		Mid R		5.43	8	-36	-19
	VI L		6.88	-20	-57	-18		VI R		5.43	33	-43	-23
	IV-V R		6.84	22	-50	-17		Pon R		5.36	6	-34	-32
	C1 R		6.81	28	-74	-35		C1 L		5.36	-33	-72	-23
	Fst L		6.76	-8	-47	-26		Pon L		5.26	-3	-34	-35
	C2 L		6.66	-23	-73	-41		IX R		5.24	10	-43	-56
	Dnt R		6.64	15	-49	-28		III R		5.24	14	-36	-27
	VI R		6.59	33	-58	-31		IX L		5.11	-9	-44	-43
	Pon R		6.58	12	-40	-33		C1 R		5.01	38	-53	-31
	VIII R		6.32	34	-55	-43		Mid L		4.96	-2	-29	-14
	VIII L		5.71	-15	-69	-49		III L		4.88	-12	-36	-26
	IX v		5.67	6	-57	-38		C2 L		4.85	-30	-89	-34
	Mid R		5.46	13	-18	-20							
	Mid L		5.45	-11	-16	-21							
	Pon L		5.36	-16	-34	-34							
	2		IPL L	2,364	5.04	-40		-44		39			

Height threshold $p < 0.001$ uncorrected for multiple correlations. Space x, y, z in mm

K_e cluster extension, Z_e equivalent Z score, *MNI* Montreal Neurological Institute space, *L* left, *R* right, Number = Cerebellar Lobule, *C* Crus, *v* Vermis, *Mid* Midbrain, *Pon* Pons, *Med* Medulla, *Dnt* Dentate, *Fst* Fastigium

Table 3 SCA and controls WM comparison

N	DARTEL	K_e	Z_e	MNI			N	SUIT	K_e	Z_e	MNI		
				x	y	z					x	y	z
1	MCP R	123,670	7.72	25	-37	-33	1	MCP R	55,685	5.93	22	-45	-30
	MCP L		7.12	-21	-55	-28		MCP L		5.70	-14	-42	-28
	SCP L		6.98	-10	-48	-36		Crs L		5.65	-9	-31	-32
	Pon R		6.12	21	-22	-35		CST R		5.47	4	-22	-32
	CST L		5.76	-26	-17	18		SCP L		5.41	-11	-48	-23
	Pon L		5.13	-2	-8	-32		ICP R		5.34	12	-51	-22
	CST R		4.25	27	-19	17		Crs R		5.29	1	-29	-27
								Mid L		5.16	-1	-19	-16
								Pon L		5.05	-14	-30	-24
								CST L		4.99	-5	-17	-31
					Pon R	4.96	16	-17	-26				

Height threshold $p < 0.001$ uncorrected for multiple correlations. Space x, y, z in mm

K_e cluster extension, Z_e equivalent Z score, *MNI* Montreal Neurological Institute, *ICP* Inferior Cerebellar Peduncle, *MCP* Middle Cerebellar Peduncle, *SCP* Superior Cerebellar Peduncle, *Crs* Pontine Crossing Tract, *CST* Corticospinal Tract, *L* left, *R* right, *Mid* Midbrain, *Pon* Pons

Supplementary Table 6). The ToL PEG correlated with a prevalently (83%) Anterior Cerebellum area of about 20,000 voxels with global maxima in $x, y, z = 31, -33, -27$ (Right Lobule IV–V near the boundary with Lobule

VI). The clusters extended more in the Right Cerebellum (68%) and included many voxels in Lobules III–VI with small parts of the Right Parahippocampal Gyrus, Crus 1, 2 and Midbrain (Supplementary Table 6). The ToL CPU

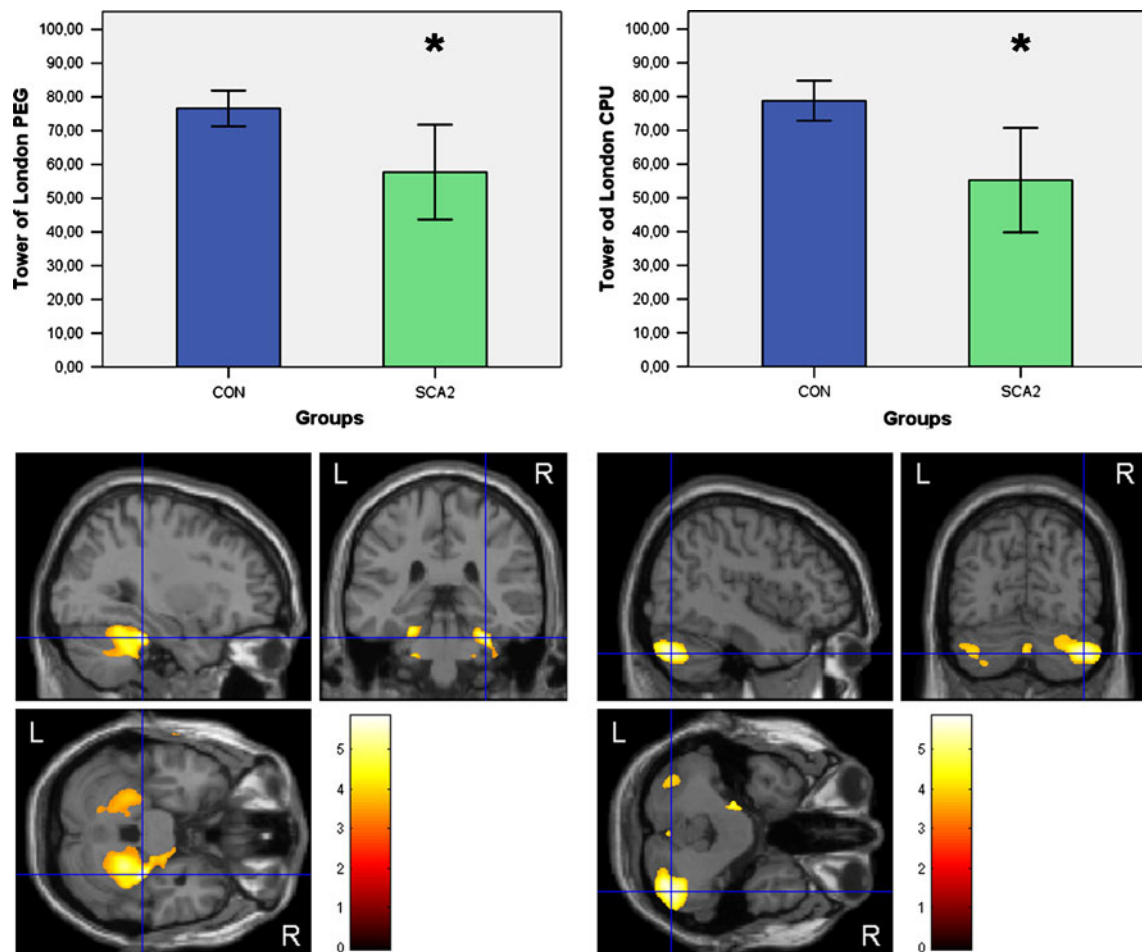


Fig. 3 Correlation between Tower of London scores and atrophy patterns. *Upper left* Traditional Tower of London scores (ToL PEG) for controls (in blue, left histogram) and SCA2 (in green, right histogram), *upper right* Computerised Tower of London scores (ToL CPU) for controls (in blue, left histogram) and SCA2 (in green, right histogram). Error bars stand for SEM, * $p < 0.05$ two independent

samples t test, ordinates units are in percent of maximum score. *Lower left* voxels volume correlated with ToL PEG, blue cross on the global maxima $x, y, z = 31, -33, -27$ mm; *Lower right* voxels volume correlated with ToL CPU, blue cross on the global maxima $x, y, z = 38, -76, -36$ mm. For all the contrasts the threshold was $p < 0.001$ uncorrected

Table 4 GM correlation with PEG and CPU

N	PEG	K_e	Z_e	MNI			N	CPU	K_e	Z_e	MNI		
				x	y	z					x	y	z
1	IV–V R	14,272	4.88	31	-33	-27	1	C1 R	8,194	4.17	38	-76	-36
2	IV–V L	5,486	4.15	-23	-33	-23	2	PHG R	7,009	4.14	22	-15	-27
							3	IV–V R	4,567	3.76	25	-40	-19
							4	IX R	1,865	3.43	10	-45	-65
							5	VIII L	1,628	3.34	-28	-53	-54
							6	C1 L	1,444	3.16	-38	-71	-36
							7	PHG L	613	3.09	-21	-19	-19

Height threshold $p < 0.001$ uncorrected for multiple correlations. Space, x, y, z in mm

K_e cluster extension, Z_e equivalent Z score, MNI Montreal Neurological Institute, PHG ParaHippocampal Gyrus, L left, R right, Number Cerebellar Lobule, C Crus

correlated with areas prevalently centred on the Posterior Cerebellum (71%) of about 25,000 voxels with global maxima in $x, y, z = 38, -76, -36$ (Right Crus 1 near the

boundary with Crus 2). The clusters extended more in the Right Cerebellum (78%) and included Lobules III–VI, Crus 1, 2, VIII, Vermis I–V, Right Hippocampus and

Parahippocampal Gyrus with small parts of Midbrain, Left Hippocampus and Parahippocampal Gyrus (Supplementary Table 6).

The correlations that survived to Finner step-down correction for multiple comparisons were reported in Supplementary Table 7. CAG repeats did not have significant corrected correlations, anyway, we reported the maximum that was $r = -0.77$ (NS) with the Inferior Cerebellar Peduncles. Age correlated significantly ($|r| > 0.80$) with some medial frontal areas, Superior Temporal Gyrus, total GM and ToL CPU (with ToL PEG the correlation was medium, $r = -0.61$, but NS). Education did not have significant correlations FDR corrected, but showed a medium $r = 0.50$ (NS) with both the ToL versions. ToL CPU and PEG showed a strong intercorrelation ($r = 0.77$), but this result would not survive to correction (NS). ICARS score; onset of disease and duration did not have any significant correlations.

We reported age and education correlations with ToL for their known effect over executive functions (Plumet et al. 2005) and the CAG repeats correlation with disease onset (-0.51 , NS) for the anticipation phenomenon in SCA2 (Schöls et al. 2004).

Discussion

Comparison with previous works

Our results reproduced very well those of Della Nave et al. (2008a, b). All their and our GM and WM atrophy's areas were the same with the exception of Corpus Callosum.

We had a partial agreement for the Corpus Callosum: we found a ROIs significance, but only with p uncorrected, and, what is more, also the authors cannot find it with VBM, emerging it only with an additional analysis with the tract-based spatial statistics (TBSS) method (Smith et al. 2006).

In their study, the R Thalamus would not be significant if they applied the threshold chosen in our work, however, this finding was interesting and in perfect agreement with Brenneis et al. (2003) and some previous neuropathological findings (Rüb et al. 2005; Rüb et al. 2003a, b, 2005). Our ROI analysis on Thalamus (Supplementary Table 5) revealed a significant lesser volume (Finner step-down corrected). This result, together with the Corticospinal Tracts and Parietal Cortex involvement, led us to assume a progressive involvement of this system and of the sensorial Thalamus with the progression of the disease. This progression could be also linked to the somatosensory and somatomotor symptoms in SCA2 (Kubis et al. 1999; Rüb et al. 2003a, b, 2005, 2007). In addition, Brenneis et al. (2003) hypothesised that the cortical and Thalamic

degeneration could start as a secondary process. This would be confirmed by the fact that a subgroup of patients with a lesser disease duration in Brenneis' work (2003) did not show any cortical atrophy (the main difference between our and Brenneis' work was the absence of cortical atrophy in our results). This fact would be confirmed also by the work of Giuffrida et al. (1999) that found a diffused cortical atrophy in their sample, but as in Brenneis study (2003) the patients had a greater number of CAG repetitions and a worse ataxia score compared to our patients. Our patients did not have dementia or forebrain global GM reduction, a feature that could be associated with a cognitive impairment, more associated with a more severe or a later stage of the disease (Klockgether et al. 1998). Taking together these observations, we could suppose that our data, together with Della Nave data (Della Nave et al. 2008a, b), were as an earlier picture of the disease evolution compared to Brenneis data.

The second work of Della Nave et al. (2008a, b) was not comparable with the previous because they used a very high conservative threshold. If we would use the same threshold we would find similar results (not shown), in fact large portions of the Cerebellum hemispheres would not appear atrophic anymore.

In the ROI analysis we found that WM is reduced also in the Inferior Occipital Fascicle, Superior Longitudinal Fascicle and Uncinate Fascicle. The involvement of these WM tracts has never been described before and allows us to suppose a more widespread WM damage in this pathology.

DARTEL and SUIT comparison

Diffeomorphic Anatomical Registration Through Exponentiated Lie Algebra and SUIT gave similar results with some differences in the extension and t values of the posterior clusters. The difference could arise from different smoothing amount employed and a good agreement in subject's alignment of the two methods. To confirm these hypothesis we estimated again the DARTEL GLM using a minor smoothing (4 mm FWHM), in fact we found an order of intensity of the peaks equal to SUIT (Right Anterior Cerebellum before Bilateral Posterior Cerebellum) and less extended clusters (data not shown).

SCA2 anatomic-clinical correlation

We did not find any correlations with ICARS, unlike previous studies (Brenneis et al. 2003; Della Nave et al. 2008a, b; Ying et al. 2006), and any correlation with disease duration or onset, like two previous studies (Brenneis et al. 2003; Della Nave et al. 2008a, b) and unlike another one (Della Nave et al. 2008a, b), both in ROIs and GLM

analyses. This result, in part, depended from the fact that the correlations reported in previous works were mild and they did not survive to the applied Finner step-down correction.

SCA2 anatomic-genetic correlation

We did not find any correlations with CAG repeats, as in previous studies in both ROIs and GLM analyses. Although the correlations did not survive to the multiple comparison correction, we wanted to indicate the strong association between Inferior Cerebellar Peduncles volume and the triplet repetitions ($r = -0.77$, $p = 0.003$). In future works, if this data will be replicated, demonstrating enough sensitivity and reliability, the volumetry of this white matter bundle could be used as a possible biomarker of CAG repetitions in SCA2.

SCA2 anatomic-neuropsychological correlations

We observed a correlation between Anterior Cerebellum and ToL PEG performance and between Posterior Cerebellum and ToL CPU. The main differences of the two tasks were that in the CPU version the sensorimotor feedbacks and skills, needed for fine coordination, were absent and on the contrary the Working Memory load was increased.

Tower of London planning task increases blood flow activity, as attested consistently by many PET and fMRI studies (e.g. Beauchamp et al. 2003; Boghi et al. 2006; Schall et al. 2003), in a network mainly composed by bilateral dorsolateral prefrontal, inferior parietal cortex and Cerebellum. These evidences converge with other theoretical, anatomical, physiological, clinical, and functional considerations that led to the incorporation of the cerebellum into the distributed neural circuits subserving cognition and emotion (Schmahmann 2010). In a recent meta-analysis (Stoodley and Schmahmann 2009), confirmed by a multiple fMRI tasks intra-subjects study (Stoodley et al. 2010), sensorimotor tasks activated the anterior Lobule IV–V and the adjacent Lobule VI. The posterior lobe was involved in higher-level tasks: executive functions activated the Lobules VI, Crus I and VIIb. These are the same areas that we observed as associated to different dysfunctions in the SCA2 patients. The dissociation between the coordinative and executive impairment was reported, regard prominence and evolution, in SCA2 patients (Le Pira et al. 2007). We hypothesise that this dissociation is linked to different areas of atrophy in the Cerebellum and that it resemble the dissociation founded in patients with cerebellar damage in different cerebellar areas (Stoodley and Schmahmann 2010). In both ToL tasks, we observed an association of the Right Cerebellum atrophy with the performances. This

result is in agreement with the hand dominance of subjects and with the involvement of the frontal left cortex in these tasks that, with Right Cerebellum is active during planning. The role of cerebellum in Working Memory is well recognised and in the recent meta-analysis (Stoodley and Schmahmann 2009) authors highlighted, as well as for executive functions, the strongest activation in the lobule VI/Crus I in both hemispheres, during verbal Working Memory tasks. The increased Working Memory load in the ToL CPU respect to the classical version, may have played a role in finding the correlation between the posterior cerebellum and the ToL CPU.

Although the two sets of areas associated with ToL versions were quite separable, the ToL CPU pattern included a part of the ToL PEG (Supplementary Fig. 16, Supplementary Table 5). At present, the scientific community is divided between embodied and disembodied theories believers, with motor representations being considered critical or merely ancillary for action and object recognition, imagery and even language understanding. The former predominantly are built on associations of deficits in these abilities whereas the latter rely on dissociations between deficits. To date, although no convincing theory is available to explain both sets of observations, cognitive neuroscientists have begun to explore an intermediate hypothesis space (Rumiati et al. 2010) that could fit well in our findings of partially overlapping and partially disjointed atrophy areas associated with different dysfunctions.

Conclusions

The correlations of different versions of the test suggested a dissociation between dysfunctions in SCA2: the Posterior Cerebellum linked to the executive dysfunction and Working Memory and the Anterior Cerebellum linked to the coordinative dysfunction. Our results could also have a clinical relevance, supporting the fact that neuropsychological classical tests, when require motor coordination, may not be adequate for the assessment of patients with movement disorders.

Acknowledgments This research was supported by Compagnia di San Paolo, “Cervelletto e cognitivita” 05-06. We wish to thank Dr. Cristina Manzone, Dr. Federica Avidano, Dr. Chiara Caroppo, Dr. Steve Valeri for their contribution to this paper, all the subjects who participated to the study and their families.

References

Andreasen NC, Rezaei K, Alliger R et al (1992) Hypofrontality in neuroleptic-naïve patients and in patients with chronic schizophrenia. Assessment with xenon 133 single-photon emission

- computed tomography and the Tower of London. *Arch Gen Psychiatry* 49:943–958
- Ashburner J (2007) A fast diffeomorphic image registration algorithm. *NeuroImage* 38(1):95–113. doi:[10.1016/j.neuroimage.2007.07.007](https://doi.org/10.1016/j.neuroimage.2007.07.007)
- Ashburner J, Friston KJ (2000) Voxel-based morphometry—the methods. *NeuroImage* 11(6 Pt 1):805–821. doi:[10.1006/nimg.2000.0582](https://doi.org/10.1006/nimg.2000.0582)
- Ashburner J, Friston KJ (2005) Unified segmentation. *NeuroImage* 26(3):839–851. doi:[10.1016/j.neuroimage.2005.02.018](https://doi.org/10.1016/j.neuroimage.2005.02.018)
- Baker SC, Rogers RD, Owen AM, Frith CD, Dolan RJ, Frackowiak RS, Robbins TW (1996) Neural systems engaged by planning: a PET study of the Tower of London task. *Neuropsychologia* 34:515–526
- Beauchamp MH, Dagher A, Aston JAD, Doyon J (2003) Dynamic functional changes associated with cognitive skill learning of an adapted version of the Tower of London task. *NeuroImage* 20(3):1649–1660. doi:[10.1016/j.neuroimage.2003.07.003](https://doi.org/10.1016/j.neuroimage.2003.07.003)
- Benjamini Y, Drai D, Elmer G, Kafkafi N, Golani I (2001) Controlling the false discovery rate in behavior genetics research. *Behav Brain Res* 125(1–2):279–284
- Bergouignan L, Chupin M, Czechowska Y, Kinkingnéhun S, Lemogne C, Le Bastard G et al (2009) Can voxel based morphometry, manual segmentation and automated segmentation equally detect hippocampal volume differences in acute depression? *NeuroImage* 45(1):29–37. doi:[10.1016/j.neuroimage.2008.11.006](https://doi.org/10.1016/j.neuroimage.2008.11.006)
- Boghi A, Rasetti R, Avidano F, Manzone C, Orsi L, D’Agata F et al (2006) The effect of gender on planning: an fMRI study using the Tower of London task. *NeuroImage* 33(3):999–1010. doi:[10.1016/j.neuroimage.2006.07.022](https://doi.org/10.1016/j.neuroimage.2006.07.022)
- Brenneis C, Bösch SM, Schocke M, Wenning GK, Poewe W (2003) Atrophy pattern in SCA2 determined by voxel-based morphometry. *Neuroreport* 14(14):1799–1802. doi:[10.1097/01.wnr.0000094105.16607.18](https://doi.org/10.1097/01.wnr.0000094105.16607.18)
- Brett M, Anton JL, Valabregue R, Poline JB (2002) Region of interest analysis using an SPM toolbox. In: 8th international conference on functional mapping of the human brain, vol 16, no 2, abstract 497. Sendai, Japan, Neuroimage
- Brusco A, Gellera C, Cagnoli C, Saluto A, Castucci A, Michielotto C et al (2004) Molecular genetics of hereditary spinocerebellar ataxia: mutation analysis of spinocerebellar ataxia genes and CAG/CTG repeat expansion detection in 225 Italian families. *Arch Neurol* 61(5):727–733. doi:[10.1001/archneur.61.5.727](https://doi.org/10.1001/archneur.61.5.727)
- Bürk K (2007) Cognition in hereditary ataxia. *Cerebellum* 6(3):280–286. doi:[10.1080/14734220601115924](https://doi.org/10.1080/14734220601115924)
- Bürk K, Globas C, Bosch S, Graber S, Abele M, Brice A et al (1999) Cognitive deficits in spinocerebellar ataxia 2. *Brain* 122(Pt 4):769–777
- Bürk K, Globas C, Bösch S, Klockgether T, Zühlke C, Daum I et al (2003) Cognitive deficits in spinocerebellar ataxia type 1, 2, and 3. *J Neurol* 250(2):207–211. doi:[10.1007/s00415-003-0976-5](https://doi.org/10.1007/s00415-003-0976-5)
- Cuingnet R, Gérardin E, Tessieras J, Auzias G, Lehéricy S, Habert MO, et al. (2010). Automatic classification of patients with Alzheimer’s disease from structural MRI: A comparison of ten methods using the ADNI database. *NeuroImage*. doi:[10.1016/j.neuroimage.2010.06.013](https://doi.org/10.1016/j.neuroimage.2010.06.013)
- Dagher A, Owen AM, Boecker H, Brooks DJ (1999) Mapping the network for planning: a correlational PET activation study with the Tower of London task. *Brain* 122:1973–1987
- Della Nave R, Ginestroni A, Tessa C, Cosottini M, Giannelli M, Salvatore E et al (2008a) Brain structural damage in spinocerebellar ataxia type 2. A voxel-based morphometry study. *Mov Disord* 23(6):899–903. doi:[10.1002/mds.21982](https://doi.org/10.1002/mds.21982)
- Della Nave R, Ginestroni A, Tessa C, Salvatore E, De Grandis D, Plasmati R et al (2008b) Brain white matter damage in SCA1 and SCA2. An in vivo study using voxel-based morphometry, histogram analysis of mean diffusivity and tract-based spatial statistics. *NeuroImage* 43(1):10–19. doi:[10.1016/j.neuroimage.2008.06.036](https://doi.org/10.1016/j.neuroimage.2008.06.036)
- Diedrichsen J (2006) A spatially unbiased atlas template of the human cerebellum. *NeuroImage* 33(1):127–138. doi:[10.1016/j.neuroimage.2006.05.056](https://doi.org/10.1016/j.neuroimage.2006.05.056)
- Diedrichsen J, Balsters JH, Flavell J, Cussans E, Ramnani N (2009) A probabilistic MR atlas of the human cerebellum. *NeuroImage* 46(1):39–46. doi:[10.1016/j.neuroimage.2009.01.045](https://doi.org/10.1016/j.neuroimage.2009.01.045)
- Dürr A (2010) Autosomal dominant cerebellar ataxias: polyglutamine expansions and beyond. *Lancet Neurology* 9(9):885–894
- Dürr A, Smadja D, Cancel G, Lezin A, Stevanin G, Mikol J, et al. (1995) Autosomal dominant cerebellar ataxia type I in Martinique (French West Indies). Clinical and neuropathological analysis of 53 patients from three unrelated SCA2 families. *Brain* 118 (Pt 6):1573–1581. <http://www.ncbi.nlm.nih.gov/pubmed/8595486>
- Eickhoff SB, Stephan KE, Mohlberg H, Grefkes C, Fink GR, Amunts K et al (2005) A new SPM toolbox for combining probabilistic cytoarchitectonic maps and functional imaging data. *NeuroImage* 25(4):1325–1335. doi:[10.1016/j.neuroimage.2004.12.034](https://doi.org/10.1016/j.neuroimage.2004.12.034)
- Estrada R, Galarraga J, Orozco G, Nodarse A, Auburger G (1999) Spinocerebellar ataxia 2 (SCA2): morphometric analyses in 11 autopsies. *Acta Neuropathol* 97(3):306–310
- Fincham JM, Carter CS, van Veen V, Stenger VA, Anderson JR (2002) Neural mechanisms of planning: a computational analysis using event-related fMRI. *Proc Natl Acad Sci USA* 99(5):3346–3351
- Finner H (1990) Some new inequalities for the Rnad distribution with application to the determination of optimum significance levels of Multiple Range Tests. *J Am Stat Assoc* 85:191–194
- Finner H (1993) On a monotonicity problem in Step-Down Multiple Test Procedures. *J Am Stat Assoc* 88:920–923
- Folstein MF, Folstein SE, McHugh PR (1975) “Mini-mental state”. A practical method for grading the cognitive state of patients for the clinician. *J Psychiatr Res* 12(3):189–198. doi:[0022-3956\(75\)90026-6](https://doi.org/10.022-3956(75)90026-6)
- Giuffrida S, Saponara R, Restivo DA, Trovato Salinaro A, Tomarchio L, Pugliares P et al (1999) Supratentorial atrophy in spinocerebellar ataxia type 2: MRI study of 20 patients. *J Neurol* 246(5):383–388
- Good CD, Johnsrude IS, Ashburner J, Henson RN, Friston KJ, Frackowiak RS (2001) A voxel-based morphometric study of ageing in 465 normal adult human brains. *NeuroImage* 14(1 Pt 1):21–36. doi:[10.1006/nimg.2001.0786](https://doi.org/10.1006/nimg.2001.0786)
- Keihaninejad S, Heckemann RA, Fagiolo G, Symms, Hajnal JV, Hammers A (2010) A robust method to estimate the intracranial volume across MRI field strengths (1.5T and 3T). *NeuroImage* 50(4):1427–1437. doi:[10.1016/j.neuroimage.2010.01.064](https://doi.org/10.1016/j.neuroimage.2010.01.064)
- Kiebel SJ, Poline JB, Friston KJ, Holmes AP, Worsley KJ (1999) Robust smoothness estimation in statistical parametric maps using standardized residuals from the general linear model. *NeuroImage* 10(6):756–766. doi:[10.1006/nimg.1999.0508](https://doi.org/10.1006/nimg.1999.0508)
- Klein A, Andersson J, Ardekani BA, Ashburner J, Avants B, Chiang MC et al (2009) Evaluation of 14 nonlinear deformation algorithms applied to human brain MRI registration. *NeuroImage* 46(3):786–802. doi:[10.1016/j.neuroimage.2008.12.037](https://doi.org/10.1016/j.neuroimage.2008.12.037)
- Klinke I, Minnerop M, Schmitz-Hübsch T, Hendriks M, Klockgether T, Wüllner U et al (2010) Neuropsychological features of patients with spinocerebellar ataxia (SCA) Types 1, 2, 3, and 6. *Cerebellum* 9(3):433–442
- Klockgether T, Ludtke R, Kramer B, Abele M, Burk K, Schöls L et al (1998) The natural history of degenerative ataxia: a retrospective study in 466 patients. *Brain* 121(Pt 4):589–600
- Kubis N, Dürr A, Gugenheim M, Chneiweiss H, Mazzetti P, Brice A et al (1999) Polyneuropathy in autosomal dominant cerebellar

- ataxias: phenotype-genotype correlation. *Muscle Nerve* 22(6):712–717
- Lazeron RH, Rombouts SA, Machielsen WC, Scheltens P, Witter MP, Uylings HB, Barkhof F (2000) Visualizing brain activation during planning: the Tower of London test adapted for functional MR imaging. *Am J Neuroradiol* 21:1407–1414
- Le Pira F, Zappala G, Saponara R, Domina E, Restivo D, Reggio E et al (2002) Cognitive findings in spinocerebellar ataxia type 2: relationship to genetic and clinical variables. *J Neurol Sci* 201(1–2):53–57. doi:[S0022510X02001946](https://doi.org/10.1007/s0022510X02001946)
- Le Pira F, Giuffrida S, Maci T, Marturano L, Tarantello R, Zappala G et al (2007) Dissociation between motor and cognitive impairments in SCA2: evidence from a follow-up study. *J Neurol* 254(10):1455–1456. doi:[10.1007/s00415-007-0548-1](https://doi.org/10.1007/s00415-007-0548-1)
- Measso G, Cavazzeran F, Zappalà G, Lebwitz BD, Crook TH, Pirozzolo FJ, Amaducci LA, Massari D, Grigoletto F (1993) The mini-mental state examination: normative study of italian random sample. *Dev Neuropsychol* 9(2):77–85
- Mori S, van Zijl P (2007) Human white matter atlas. *Am J Psychiatr* 164(7):1005. doi:[10.1176/appi.ajp.164.7.1005](https://doi.org/10.1176/appi.ajp.164.7.1005)
- Morris RG, Ahmed S, Syed GM (1993) Neural correlates of planning ability: frontal lobe activation during the Tower of London test. *Neuropsychologia* 31:1367–1378
- Nardacchione A, Orsi L, Brusco A, Franco A, Grosso E, Dragone E et al (1999) Definition of the smallest pathological CAG expansion in SCA7. *Clin Genet* 56(3):232–234
- Newman SD, Carpenter PA, Varma S, Just MA (2003) Frontal and parietal participation in problem solving in the Tower of London: fMRI and computational modeling of planning and high-level perception. *Neuropsychologia* 41(12):1668–1682
- Orsi L, D'Agata F, Caroppo P, Franco A, Caglio MM, Avidano F et al (2010) Neuropsychological picture of 33 spinocerebellar ataxia cases. *Journal of Clinical and Experimental Neuropsychology*. 33:315–325. doi:[10.1080/13803395.2010.518139](https://doi.org/10.1080/13803395.2010.518139)
- Pang JT, Giunti P, Chamberlain S, An SF, Vitaliani R, Scaravilli T et al (2002) Neuronal intranuclear inclusions in SCA2: a genetic, morphological and immunohistochemical study of two cases. *Brain* 125(Pt 3):656–663
- Pell GS, Briellmann RS, Chan CHP, Pardoe H, Abbott DF, Jackson GD (2008) Selection of the control group for VBM analysis: influence of covariates, matching and sample size. *NeuroImage* 41(4):1324–1335. doi:[10.1016/j.neuroimage.2008.02.050](https://doi.org/10.1016/j.neuroimage.2008.02.050)
- Pereira JMS, Xiong L, Acosta-Cabrero J, Pengas G, Williams GB, Nestor PJ (2010) Registration accuracy for VBM studies varies according to region and degenerative disease grouping. *NeuroImage* 49(3):2205–2215. doi:[10.1016/j.neuroimage.2009.10.068](https://doi.org/10.1016/j.neuroimage.2009.10.068)
- Plumet J, Gil R, Gaonac'h D (2005) Neuropsychological assessment of executive functions in women: effects of age and education. *Neuropsychology* 19(5):566–577. doi:[10.1037/0894-4105.19.5.566](https://doi.org/10.1037/0894-4105.19.5.566)
- Rasser PE, Johnston P, Lagopoulos J, Ward PB, Schall U, Thienel R et al (2005) Functional MRI BOLD response to Tower of London performance of first-episode schizophrenia patients using cortical pattern matching. *NeuroImage* 26:941–951
- Rüb U, Del Turco D, Del Tredici K, de Vos RAI, Brunt ER, Reifenberger G et al (2003a) Thalamic involvement in a spinocerebellar ataxia type 2 (SCA2) and a spinocerebellar ataxia type 3 (SCA3) patient, and its clinical relevance. *Brain* 126(Pt 10):2257–2272. doi:[10.1093/brain/awg234](https://doi.org/10.1093/brain/awg234)
- Rüb U, Schultz C, Del Tredici K, Gierga K, Reifenberger G, de Vos RAI et al (2003b) Anatomically based guidelines for systematic investigation of the central somatosensory system and their application to a spinocerebellar ataxia type 2 (SCA2) patient. *Neuropathol Appl Neurobiol* 29(5):418–433
- Rüb U, Del Turco D, Bürk K, Diaz GO, Auburger G, Mittelbronn M et al (2005) Extended pathoanatomical studies point to a consistent affection of the thalamus in spinocerebellar ataxia type 2. *Neuropathol Appl Neurobiol* 31(2):127–140. doi:[10.1111/j.1365-2990.2004.00617.x](https://doi.org/10.1111/j.1365-2990.2004.00617.x)
- Rüb U, Seidel K, Ozerden I, Gierga K, Brunt ER, Schöls L et al (2007) Consistent affection of the central somatosensory system in spinocerebellar ataxia type 2 and type 3 and its significance for clinical symptoms and rehabilitative therapy. *Brain research reviews* 53(2):235–249. doi:[10.1016/j.brainresrev.2006.08.003](https://doi.org/10.1016/j.brainresrev.2006.08.003)
- Rumiati RI, Papeo L, Corradi-Dell'Acqua C (2010) Higher-level motor processes. *Ann N Y Acad Sci* 1191(1):219–241. doi:[10.1111/j.1749-6632.2010.05442.x](https://doi.org/10.1111/j.1749-6632.2010.05442.x)
- Schall U, Johnston P, Lagopoulos J, Jüptner M, Jentzen W, Thienel R et al (2003) Functional brain maps of Tower of London performance: a positron emission tomography and functional magnetic resonance imaging study. *NeuroImage* 20(2):1154–1161. doi:[10.1016/S1053-8119\(03\)00338-0](https://doi.org/10.1016/S1053-8119(03)00338-0)
- Schmahmann JD (2010) The role of the cerebellum in cognition and emotion: personal reflections since 1982 on the dysmetria of thought hypothesis, and its historical evolution from theory to therapy. *Neuropsychol Rev* 20(3):236–260. doi:[10.1007/s11065-010-9142-x](https://doi.org/10.1007/s11065-010-9142-x)
- Schmahmann JD, Doyon J, McDonald D, Holmes C, Lavoie K, Hurwitz AS et al (1999) Three-dimensional MRI atlas of the human cerebellum in proportional stereotaxic space. *NeuroImage* 10(3 Pt 1):233–260. doi:[10.1006/nimg.1999.0459](https://doi.org/10.1006/nimg.1999.0459)
- Schmitz-Hübsch T, Tezenas du Montcel S, Baliko L, Boesch S, Bonato S, Fancellu R et al (2006) Reliability and validity of the International Cooperative Ataxia Rating Scale: a study in 156 spinocerebellar ataxia patients. *Mov Disord* 21(5):699–704. doi:[10.1002/mds.20781](https://doi.org/10.1002/mds.20781)
- Schöls L, Bauer P, Schmidt T, Schulte T, Riess O (2004) Autosomal dominant cerebellar ataxias: clinical features, genetics, and pathogenesis. *Lancet Neurol* 3(5):291–304. doi:[10.1016/S1474-4422\(04\)00737-9](https://doi.org/10.1016/S1474-4422(04)00737-9)
- Shallice T (1982) Specific impairments of planning. *Philos Trans R Soc Lond B Biol Sci* 298(1089):199–209
- Smith SM, Jenkinson M, Johansen-Berg H, Rueckert D, Nichols TE, Mackay CE et al (2006) Tract-based spatial statistics: voxelwise analysis of multi-subject diffusion data. *NeuroImage* 31(4):1487–1505. doi:[10.1016/j.neuroimage.2006.02.024](https://doi.org/10.1016/j.neuroimage.2006.02.024)
- Soong BW, Paulson HL (2007) Spinocerebellar ataxias: an update. *Curr Opin Neurol* 20(4):438–446. doi:[10.1097/WCO.0b013e3281fbd3dd](https://doi.org/10.1097/WCO.0b013e3281fbd3dd)
- Stoodley CJ, Schmahmann JD (2009) Functional topography in the human cerebellum: a meta-analysis of neuroimaging studies. *NeuroImage* 44(2):489–501. doi:[10.1016/j.neuroimage.2008.08.039](https://doi.org/10.1016/j.neuroimage.2008.08.039)
- Stoodley CJ, Schmahmann JD (2010) Evidence for topographic organization in the cerebellum of motor control versus cognitive and affective processing. *Cortex* 46(7):831–844. doi:[10.1016/j.cortex.2009.11.008](https://doi.org/10.1016/j.cortex.2009.11.008)
- Stoodley CJ, Valera EM, Schmahmann JD (2010) An fMRI study of intra-individual functional topography in the human cerebellum. *Behav Neurol* 23(1–2):65–79. doi:[10.3233/BEN-2010-0268](https://doi.org/10.3233/BEN-2010-0268)
- Trouillas P, Takayanagi T, Hallett M, Currier RD, Subramony SH, Wessel K et al (1997) International Cooperative Ataxia Rating Scale for pharmacological assessment of the cerebellar syndrome. The Ataxia Neuropharmacology Committee of the World Federation of Neurology. *J Neurol Sci* 145(2):205–211. doi:[S0022510X96002316](https://doi.org/10.1016/S0022510X96002316)
- Tzourio-Mazoyer N, Landeau B, Papathanassiou D, Crivello F, Etard O, Delcroix N et al (2002) Automated anatomical labeling of activations in SPM using a macroscopic anatomical parcellation of the MNI MRI single-subject brain. *NeuroImage* 15(1):273–289. doi:[10.1006/nimg.2001.0978](https://doi.org/10.1006/nimg.2001.0978)

- Van den Heuvel OA, Groenewegen HJ, Barkhof F, Lazeron RHC, van Dyck R, Veltman DJ (2003) Frontostriatal system in planning complexity: a parametric functional magnetic resonance version of Tower of London task. *NeuroImage* 18:367–374
- Ying SH, Choi SI, Perlman SL, Baloh RW, Zee DS, Toga AW (2006) Pontine and cerebellar atrophy correlate with clinical disability in SCA2. *Neurology* 66(3):424–426. doi:[10.1212/01.wnl.0000196464.47508.00](https://doi.org/10.1212/01.wnl.0000196464.47508.00)
- Zung WW (1965) A Self-Rating Depression Scale. *Arch Gen Psychiatry* 12:63–70